

## COMPARISON BETWEEN FINITE ELEMENT PREDICTIONS AND NOTCH CONVERSION RULE ESTIMATES FOR TWO DIMENSIONAL AND AXISYMMETRIC COMPONENTS

### **M. K. Pipelzadeh**

Department of Mechanical Engineering, University of Wales, Swansea, SA2 8PP, UK,  
e-mail: m.k.pipelzadeh@swansea.ac.uk

### **S. J. Hardy**

Department of Mechanical Engineering, University of Wales, Swansea, SA2 8PP, UK,  
e-mail: s.j.hardy@swansea.ac.uk

### **A. R. Gowhari-Anaraki**

Department of Mechanical Engineering, University of Science and Technology, Tehran, Iran

***Abstract.** This paper compares finite element predictions of strain and strain range with estimates obtained from simple notch stress-strain conversion (NSSC) rules. A wide range of two dimensional and axisymmetric components were considered, including data from other published analyses, in order to verify the suitability of the NSSC rules. The elastic-plastic comparisons are made for various loading conditions (i.e., monotonic and cyclic) and geometries using the elastic-perfectly-plastic (EPP) material model. The NSSC rules were found to overestimate the finite element predictions and they are generally dependent on both the geometry and load level. Similar findings have been noted in some of the published papers.*

***Keywords:** Neuber, notch, finite element, elastic plastic analysis.*

## **1. INTRODUCTION**

Most engineering components contain geometric discontinuities, with abrupt changes in the cross section. These including projections, holes, grooves, threads, flanges, etc., and these induce local high stresses. These stress raisers are generally termed notches and are likely places for plastic deformation under moderate to high loading. The latter condition may result in fatigue crack initiation (FCI) and subsequent propagation at the roots of these notches. Therefore, the designer must consider these effects in particular for components under variable or cyclic loading.

Elastic stress concentration factors (SCFs), defined as the maximum localised stress at the notch to the nominal stress away from the discontinuity, are useful data particularly for components made from brittle materials. However, for components made from ductile materials, which may experience significant yielding, the local strain approach is more appropriate to predict the design life of notched components. This is discussed in detail by Dowling et al.(1977) particularly for low cycle fatigue (LCF) conditions. This approach requires an estimate of the local strain range at the notch. FCI life predictions for notched components are based on the local strain approach and fatigue data obtained from simple

uniaxial unnotched specimen tests, where it is assumed that smooth and notched specimens with the same local strain range experience the same number of cycles to failure. The local strain range can be obtained by the following three methods:

- (1) prototype component testing,
- (2) elastic-plastic finite element analysis or other numerical or analytical prediction methods,
- (3) notch stress-strain conversion (NSSC) rules.

Methods (2) and (3) are analytical approaches for predicting the non-linear and history-dependent stress-strain behaviour of the notch root in terms of the load history and the cyclic deformation properties of the metal. Method (1) can be very expensive and time consuming.

Although finite element analysis is a very powerful technique, elastic-plastic analysis is much more complex than elastic analysis, especially when the components have complicated geometries and/or loading conditions. The NSSC rules, on the other hand, provide a relatively simple method of estimating local strains which can then be used to obtain an FCI life prediction for the notched component using either smooth specimen fatigue life data or other standard numerical relationships (e.g. Manson-Coffin (1954)). The most well-known NSSC rules are Neuber, Linear, Hardrath-Ohman and Intermediate (see Reference by Fuchs and Stephen (1980)). Extensive studies concerning the experimental and analytical verification of these rules for a wide range of geometries have been performed by a number of researchers and a review of the relevant work is given by Gowhari-Anaraki and Hardy (1991).

Loaded projections on two dimensional (2D), axisymmetric and three dimensional (3D) components (i.e., refer to components where the load is applied or reacted close to the geometric discontinuity) are often used to transmit a variety of loading between two or more parts. Typical applications include bolted joints, turbine blade roots, lifting lugs, connecting collars, shouldered plates and anchorage points for machinery parts. Stress levels induced in the vicinity of the projection can be very high and low cycle fatigue, under variable loading, is a potential mechanism for ultimate failure. Even when loads or reactions are applied 'remotely' from the projection, the presence of that projection will have a decisive effect on the stress field and low cycle fatigue failure is, again, possible.

Both 2D (e.g., in the form of flat 'T' shaped plates) and axisymmetric components (e.g., hollow tube with internal projections) have been the subject of detailed elastic and elastic-plastic analyses by Hardy and Gowhari-Anaraki (1993) and Hardy and Pipelzadeh (1996) respectively in order to assess the suitability of the NSSC rules. In this paper, 2D and axisymmetric components subjected to shear and axial loading respectively are considered. Emphasis is given to the Neuber and Intermediate rules associated to the 2D and 3D components respectively using EPP material model. In addition, some previously published experimental and numerical results for other 2D and axisymmetric problems are compared with NSSC rule estimates and the findings discussed in association with the findings from the current work.

## **2. BACKGROUND**

### **2.1 NSSC rules**

As previously mentioned in Section 1, components under intermediate and, to a large extent, low cycle fatigue will experience significant yielding. In these regions, the plastic stress concentration factor,  $K_{\sigma}$ , and the elastic-plastic strain concentration factor,  $K_{\epsilon}$ , are no longer

equal to the elastic stress concentration factor,  $K_t$ . Beyond yielding,  $K_\epsilon$  increases with the load while  $K_\sigma$  decreases.

Several relationships between these factors have been proposed, referred here as the NSSC rule estimates. For 2D components, the Neuber rule is normally associated with plane stress problems (e.g., thin plates such as the flat 'T' shaped component) while the Linear rule is associated to the plane strain problems (e.g., thick plates). However, for 3D or axisymmetric components, the Intermediate rule has been considered since it lies between these two extreme conditions.

### *Neuber rule*

$$K_t^2 = K_\sigma K_\epsilon = \frac{\hat{\sigma}}{\sigma_a} \frac{\hat{\epsilon}}{\epsilon_a} \quad \text{.....(1)}$$

or  $\hat{\sigma}\hat{\epsilon} = K_t^2 \sigma_a \epsilon_a = \text{Constant}$  (monotonic loading) .....(2)

and  $\Delta\hat{\sigma}\Delta\hat{\epsilon} = K_t^2 \Delta\sigma_a \Delta\epsilon_a = \text{Constant}$  (cyclic loading) .....(3)

where  $\hat{\sigma}, \hat{\epsilon}$  are local peak stress and strain at the notch respectively and  $\sigma_a, \epsilon_a$  are nominal stress and strain measured remotely from the notch,  $\Delta$  refers to the amplitude or range (i.e., the peak-to-peak change during one load reversal or half cycle).

### *Intermediate rule*

$$\frac{K_\epsilon}{K_t} = \left(\frac{K_t}{K_\sigma}\right)^I \quad \text{.....(4)}$$

or  $I = \frac{\log(K_\epsilon / K_t)}{\log(K_t / K_\sigma)}$  .....(5)

When index 'I' is set equal to 1, it corresponds to the Neuber rule which generally applies to plane stress problems whereas when index 'I' = 0, it gives the other extreme condition, which is the Linear rule (i.e.,  $K_t = K_\epsilon$ ) for plane strain or thick plate problems. In this investigation the index 'I' is set equal to 0.5 for the axisymmetric component as established by Gowhari-Anaraki and Hardy (1991).

The above equations can be modified for multi-axial states of stress using various methods (see Reference by Miller and Brown (1985)). For the 2D component being considered here, the dominant stress component is the meridional stress (i.e., parallel to the free surface). However, the axisymmetric component is subjected to multiaxial-states of stress with the meridional stress component, again, being the dominant component and to less extent the hoop and radial stresses (for details refer to Fig. 2 of Hardy and Gowhari-Anaraki (1989)). Therefore, for 2D component, the meridional stress and strain are considered whereas for the axisymmetric component the equivalent stress (i.e., based on von Mises) and equivalent total strain are used. Therefore, Eq. (4) can be expressed in terms of stress and strain components as follows:

$$\hat{\sigma}_{eq}^I \hat{\epsilon}_{eq}^I = K_{teq}^{(I+1)} \sigma_a^I \epsilon_a \quad \text{(monotonic loading)} \quad \text{.....(6)}$$

$$\text{and } \Delta \hat{\sigma}_{eq}^I \Delta \hat{\epsilon}_{eq}^t = K_{teq}^{(I+1)} \Delta \sigma_a^I \Delta \epsilon_a \quad (\text{cyclic loading}) \quad \dots(7)$$

where,  $K_{teq}$  referred to as the maximum equivalent stress index.

### 3. COMPONENT GEOMETRIES, LOADING & BOUNDARY CONDITIONS AND MATERIAL MODEL

The basic geometric parameters of the 2D and axisymmetric components are shown in Fig. 1. Load applications and reactions are clearly shown in the figure. Loads are expressed using a normalised load parameters,  $\lambda$  and  $\gamma$  for 2D and axisymmetric components respectively:

$$\begin{aligned} \lambda &= \text{nominal shear stress in the shank/yield shear stress} \\ &= \frac{\tau_a}{\tau_y} \end{aligned} \quad \dots(8)$$

where  $\tau_y = \sigma_y/2$

$$\text{and } \tau_a = Q/\text{area} = Q/ds \quad \dots(9)$$

where  $Q$  is the transverse shear load,  $d$  and  $s$  are the shank depth and thickness respectively.

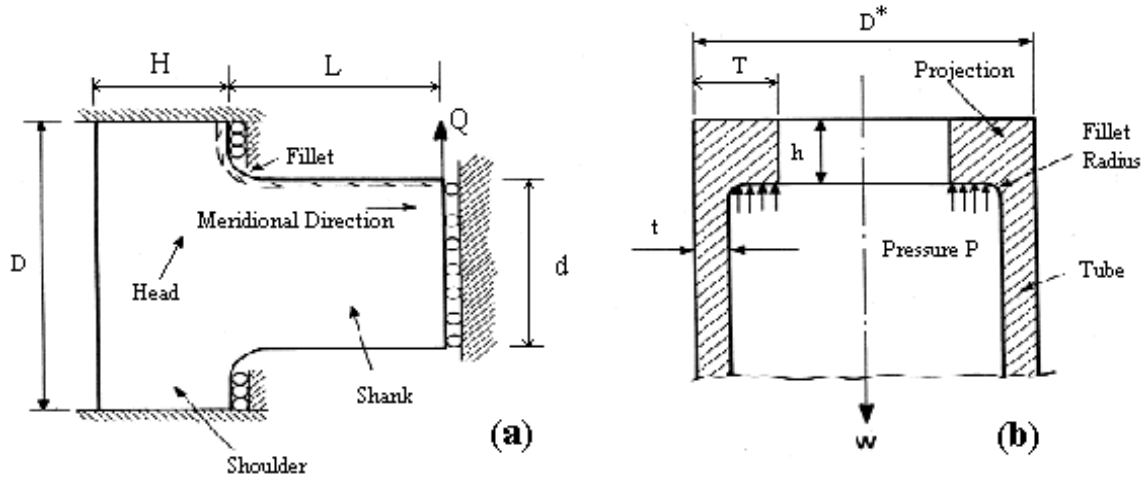


Figure 1- Geometries for (a) 2 D and (b) axisymmetric components.

Similarly,  $\gamma = \text{nominal axial stress in the tube/yield stress}$

$$= \frac{\sigma_a}{\sigma_y} \quad \dots(10)$$

$$\text{where } \sigma_a = \frac{W}{\pi t(D^* - t)} = E\epsilon_a \quad \dots(11)$$

and  $W$  is the applied axial load,  $D^*$  and  $t$  are the tube outside diameter and thickness respectively and  $E$  is the elastic modulus.

The elastic-plastic stress-strain behaviour of the components has been modelled throughout using a simple bilinear time-independent elastic-perfectly-plastic (EPP) material model.

## 4. RESULTS

### 4.1 Monotonic loading

All the results are taken at the worst Gauss points nearest to the free surface in the fillet region. Maximum peak fillet stress and strain indices (i.e.,  $K_t$ ,  $K_\sigma$  and  $K_\epsilon$ ) are obtained by dividing the stress and strain predictions by the respective nominal values at the uniform section (i.e.,  $K_t = \hat{\sigma} / \sigma_a$ ).

Figure 2(a) and (b) show the variation of  $K_\sigma$  and  $K_\epsilon$  for the 2D and axisymmetric components respectively with the nominal loads  $\lambda$  and  $\gamma$ . The main observations are:

(i) the normalised stress curves (i.e.,  $K_\sigma$  vs.  $\lambda$  and  $\gamma$ ) for both components are approximately the same and are independent of geometry (i.e.,  $K_t$ ). Below these curves, the behaviour of the components is purely elastic. The onset of yielding, is represented by the curve:

$$\text{i.e., } K_\sigma = K_t \quad \dots(12)$$

and at these points, the loading parameters,  $\lambda$  and  $\gamma$ , are approximately equal to the reciprocal of  $K_t$ .

$$\text{i.e., } \lambda = \gamma = 1/K_t \quad (\text{at yield}) \quad \dots(13)$$

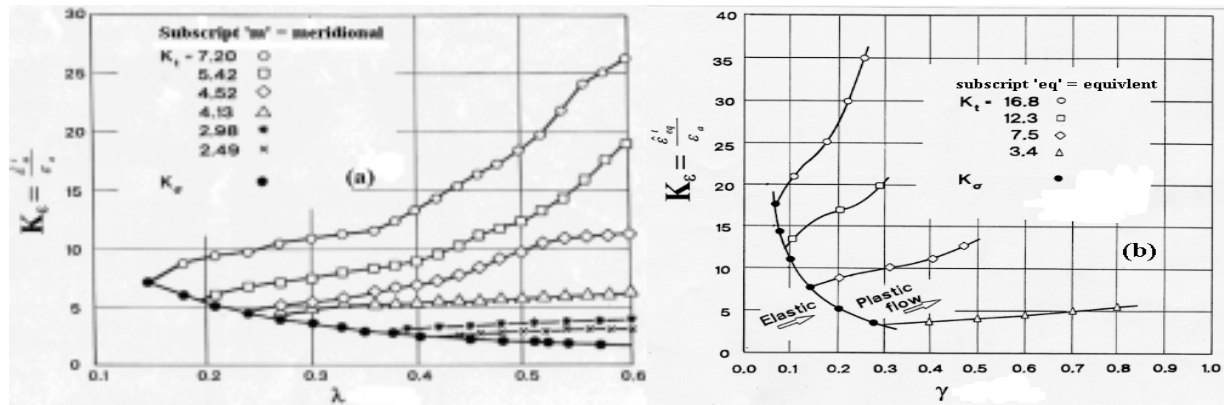


Figure 2- Variation of  $K_\epsilon$ ,  $K_\sigma$  with  $\lambda$  and  $\gamma$  for (a) 2D and (b) axisymmetric components under monotonic loading.

(ii) beyond the elastic limit, where plastic flow occurs, there is an increase in  $\hat{\epsilon}^t / \epsilon_a$  (i.e.,  $K_\epsilon$ ) with increasing of load parameter coupled with a reduction in  $K_\sigma$ . Obviously, for geometries with high  $K_t$  value, the onset of yielding will occur at lower load levels.

## 4.2 Repeated loading

The results are in the form of normalised stress and strain ranges. These are obtained by dividing the predicted stress and strain range values by the corresponding nominal values (i.e.,  $\Delta\sigma_a$  and  $\Delta\varepsilon_a$ ). Thus, normalised meridional and equivalent stress range are equal to  $\Delta\hat{\sigma}_m / \Delta\sigma_a$  and  $\Delta\hat{\sigma}_{eq} / \Delta\sigma_a$  respectively. Similarly, normalised meridional and equivalent total strain range are equal to  $\Delta\hat{\varepsilon}_m^t / \Delta\varepsilon_a$  and  $\Delta\hat{\varepsilon}_{eq}^t / \Delta\varepsilon_a$  respectively.

Figure 3(a) and (b) show the variation of  $K_\varepsilon$  and  $K_\sigma$  with nominal loads  $\lambda$  and  $\gamma$  for the 2D and axisymmetric components respectively. The general trends are similar to those described in Section 4.1. Under repeated loading, the normalised stress and strain ranges initially remain equal to  $K_t$  (i.e., elastic) if no compressive yielding occurs upon unloading.

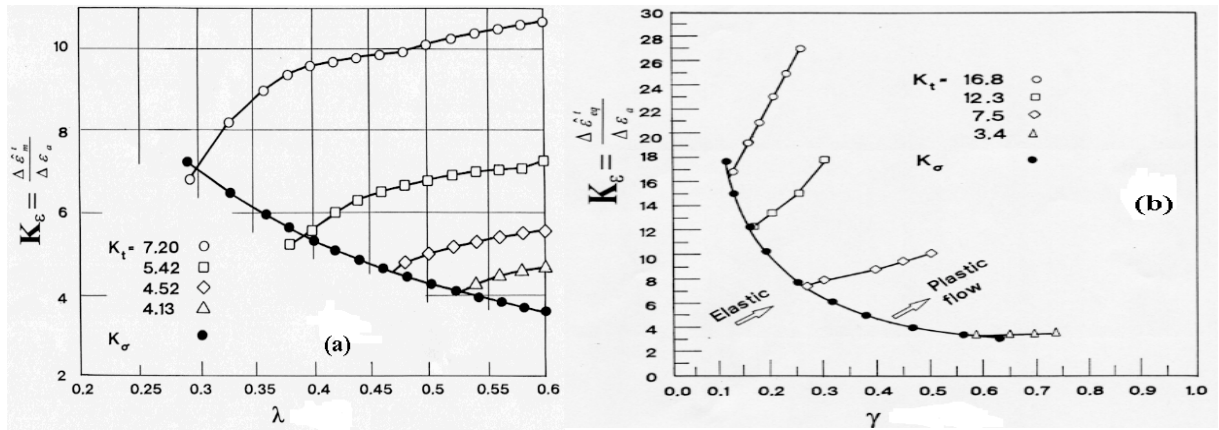


Figure 3- Variation of  $K_\varepsilon$ ,  $K_\sigma$  with  $\lambda$  and  $\gamma$  for (a) 2D and (b) axisymmetric components under repeated loading.

However, above a certain limiting nominal stress, compressive yielding will occur during unloading and further increases in nominal stress result in a reduction in  $K_\sigma$  and an increase in  $K_\varepsilon$ . For 2D component, slight discrepancies between  $K_\sigma$  and  $K_\varepsilon$  at initial yielding are obtained, particularly for components with large SCF,  $K_t$ . These are caused by other stress tensors, identified by Pipelzadeh and Hardy (1997), (i.e., shear stress term, which is significant in the short beams). However, for the axisymmetric component, the triaxial states-of-stress and strain, at yield, are accounted for in the equivalent stress and strain terms and are, therefore, equal in magnitude (i.e.,  $(\sigma_{eq})_y = (\varepsilon_{eq})_y E$ ).

Figure 3 clearly shows that the onset of compressive yielding,  $K_\sigma$ , remains equal to  $K_t$ , as previously identified in eq. (12) for monotonic loading. However,  $K_t$  is now equal to twice the nominal load level. This is because reverse yielding occurs when the stress range is twice the yield stress. This can be expressed as:

$$\lambda = \gamma = 1/2K_t \quad (\text{at yield}) \quad \dots(14)$$

## 4.3 NSSC rule estimates

In this section, the predicted strain and strain ranges are compared with the simple NSSC rules for a variety of load conditions. The deviation between the NSSC rule estimates and finite element predictions is expressed by the follow equation:

$$\text{Deviation (N)} = \text{NSSC rule estimates/finite element predictions} \quad \dots(15)$$

The load levels are expressed in terms of yield stress,  $\sigma_y$ , within the range  $1.1 < \sigma_y < 3.0$ .

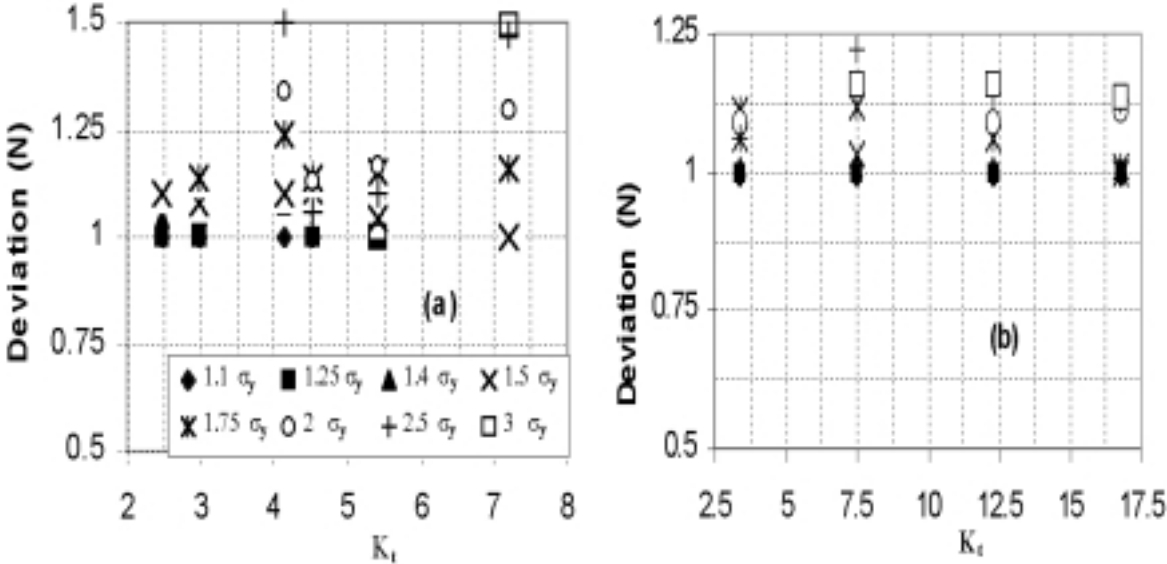


Figure 4- The deviation between NSSC rule estimates and finite element predictions with  $K_t$  for (a) 2D and (b) axisymmetric components under monotonic shear & axial loads (expressed in terms of yield stress,  $\sigma_y$ ).

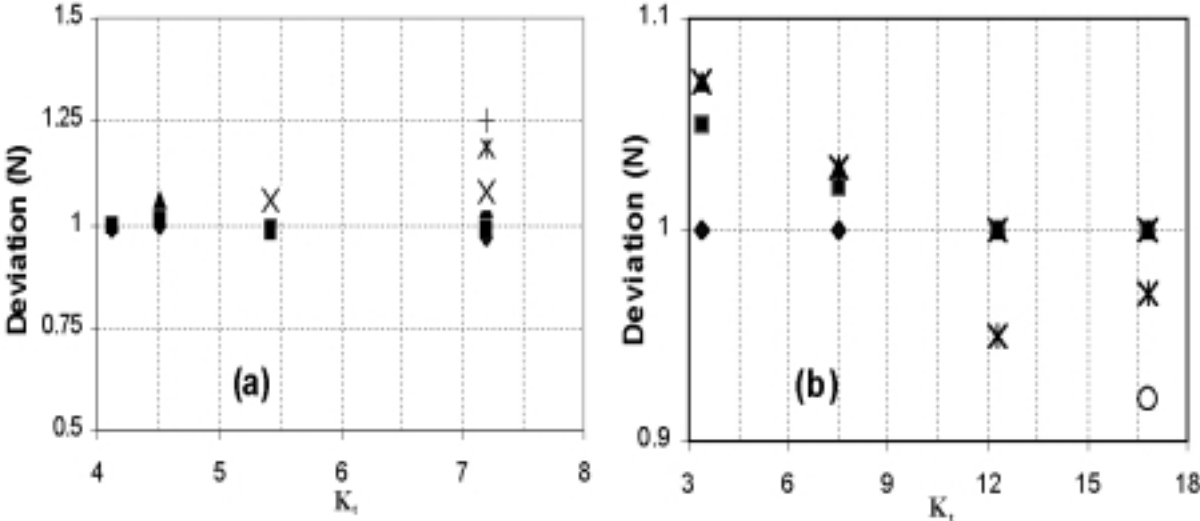


Figure 5- The deviation between NSSC rule estimates and finite element predictions with  $K_t$  for (a) 2D and (b) axisymmetric components under repeated shear & axial loads (expressed in terms of yield stress,  $\sigma_y$ , see Fig. 4 for notations).

Figure 4(a) and (b) show the deviations for the 2D and axisymmetric components under monotonic loading. The degree of scatter in the results is clearly evident in particular in Fig. 4(a) for components with large  $K_t$  values and high nominal loads. However, for low to moderate loads above yielding, the Neuber (for 2D) and Intermediate (for axisymmetric) rules give reasonable estimates. The overall results show that both rules overestimate the finite element predictions with the average values of  $N=1.1$  and  $N= 1.06$  for 2D and axisymmetric components respectively, hence the NSSC rules are conservative.

For repeated loading, the degree of scatter is much lower than for monotonic loading as shown in Fig. 5. This is because the components are subjected to lower nominal loads and therefore produced less gross yielding. Average values of  $N=1.04$  and  $1.01$  are obtained for 2D and axisymmetric components respectively with both pessimistic and optimistic estimates being obtained.

#### 4.4 Summary of results of other published data

A summary of a number of investigations (experimental and numerical) is presented in Table 1 for 2D and axisymmetric components in order to confirm the suitability and the accuracy of the NSSC rule estimates. The deviation,  $N$ , has been determined here on the basis of the stress and strain data presented by these authors. The results show that the NSSC rules are generally conservative for a wide range of geometries and loadings. The few cases where the NSSC rules are optimistic yield values close to unity.

Table 1- Data for other published work.

References	Component/loading	$K_t$	$K_e$	$K_G$	Deviation 'N'	Remarks
Hoffman and Seeger (1985)	Circumferential notched round bar. Cyclic push-pull ( <b>Axisymmetric</b> )	3.27	3.75 4.62 5.88 7.00	2.5 1.53 1.18 1.00	1.00 1.03 0.93 0.85	Finite element predictions with EPP material model
Hardy (1983)	Flanged tube. Axial + Thermal loading ( <b>Axisymmetric</b> )	1.38	1.40	1.11	1.10	Finite element predictions with multi-linear hardening. Results compare well with experiment (ERS gauges)
Fessler and Wilson (1964)	Flat step bar. Axially loaded projection ( <b>Axisymmetric</b> )	2.24 6.20	2.39 8.46	1.72 1.68	1.07 1.41	Results by experiment (photoelasticity)
Kotani et al. (1976)	Side notched plate. Cyclic push-pull ( <b>2 D</b> )	2.00 2.60 2.30	2.20 3.38 2.62	1.80 2.03 1.89	1.00 0.99 1.07	Results by experiment (ERS gauges)
Gowda and Topper (1970)	Infinite plate with circular and elliptical holes. ( <b>2 D</b> )	2.54 2.72 3.82 4.12	3.50 3.83 6.60 7.83	1.77 1.74 1.76 1.74	1.04 1.11 1.26 1.25	Results by experiment for nominal stress = 30 ksi (See Fig. 7 and 8)
Papirno (1971)	Flat notched tensile strips. ( <b>2D</b> )	1.50 1.59 2.00	- - -	- - -	1.10 1.02 1.14	Experimental results. The deviations are obtained from Fig. 6,7 & 8 at notch stress = 160 ksi



## 5. CONCLUSION

In this study, the behaviour of a range of geometries and loading conditions using an EPP material model (which represents the extreme condition in terms of strain) have been considered for two typical cases of components with projections. The overall finite element strain and strain range predictions compared favourably with the NSSC rule estimates (i.e., Neuber rule which is normally associated with plane stress problems, and Intermediate rule, with index  $I=0.5$ , for axisymmetric components), in particular at low to moderate load levels. However, at high load levels, which result in excessive yielding, both the NSSC rules provided the upper bound and therefore give conservative fatigue life predictions. For both components,  $K_{\sigma}$  was found to be independent of geometry. Similar findings have been observed by analysing the results from a number of researchers for other 2D and axisymmetric components.

## 6. REFERENCES

- Coffin Jr, L. F., 'A study of the effects of cyclic thermal stresses on a ductile metal', Trans. ASME, 1954, 76, pp. 931-950.
- Dowling, N. E., Brose, W. R. and Wilson, W. K., 'Notched member fatigue life prediction by the local strain approach', in Advances in Engineering, edited by R. M. Wetzell, Vol. 6, 1977 (Society of Automotive Engineers, New York), p. 57.
- Fessler, H. and Wilson, R. W., 'Plastic-elastic strains observed near loaded fillets in stepped bars', J. Mech. Eng. Sciences, Vol. 6, No. 1, 1964.
- Fuchs, H. O., Stephens, R. I., Metal Fatigue in Engineering, John Wiley and Sons, New York, 1980
- Gowda, C. V. B. & Topper, T. H. 'On the relation between stress and strain concentration factors in notched members in plane stress', Trans. ASME, J. Applied Mechanics, 1970, 37, pp. 77-84.
- Gowhari-Anaraki, A. R and Hardy, S. J. , 'Low cycle fatigue life predictions for hollow tubes with axially loaded axisymmetric internal projections', J. Strain Analysis, 1991, Vol. 26, pp. 133-146.
- Hardy, S. J. and Gowhari-Anaraki, A. R., 'Stress concentration factors and elastic - plastic stress and strain predictions for axisymmetric internal projections on hollow tubes subjected to axial loading', J. Strain Analysis, 1989, Vol. 24, pp. 45-54.
- Hardy, S. J. and Gowhari-Anaraki, A. R., 'Stress and strain range predictions for axisymmetric and two-dimensional components with stress concentrations and comparisons with notch stress-strain conversion rule estimates', J. Strain Analysis, 1993, Vol. 28(3), pp. 209-221.
- Hardy, S. J. and Pipelzadeh, M. K., 'An assessment of the notch stress-strain conversion rules for short flat bars with projections subjected to axial and shear loading', J. Strain Analysis, 1996, Vol. 31(2), pp. 91-110.
- Hardy, S. J. 'Finite element analysis of components subjected to ratchetting and creep', PhD Thesis, University of Nottingham, 1983.
- Hoffman, M. & Seeger, T. , 'A generalized method for estimating multiaxial elastic-plastic notch stresses and strains', Parts I and II, Journal Engineering Masters Technology, 1985, 107, 250-260.
- Kotani, S., Koibuchi, K. & Kasai, K., 'The effect of notches on cyclic stress strain behaviour and fatigue crack initiation', Proceedings of the 2<sup>nd</sup> Conference on Mechanical Behaviour of Materials, 1976, pp. 606-610.
- Miller, K. J. & Brown, M. W., Multiaxial Fatigue, ASTM STP 853, 1985 (American Society for Testing and Materials, Philadelphia, Pa.), pp. 553-634.

- Papirno, R., 'Plastic stress strain history at notch roots in tensile strips under monotonic loading', *Experimental Mechanics*, 1971, pp. 446-452.
- Pipelzadeh, M. K. & Hardy, S. J., 'Stress prediction for short flat bars with projections subjected to shear loading', 14<sup>th</sup> Brazilian Congress of Mechanical Engineering, 1997, COB 103.